Electronic structure of magnetic ternary alkali metal–manganese hydrides

Emilio Orgaz
Departamento de Física y Química Teórica, Facultad de Química, Universidad Nacional Autónoma de México, CP 04510, Coyoacán, México, Distrito Federal, Mexico

(Received 15 July 1999; revised manuscript received 18 October 1999)

Magnetic ternary alkali metal–manganese-based hydrides have recently been discovered. These hydrides show an antiferromagnetic order transition at low temperatures. We have investigated the electronic structure, chemical bonding, and magnetic moment of such materials, by means of the full-potential linear-augmented-plane-wave method. The corresponding isostructural manganese halide has been also considered. We found that these materials are all semiconductors that show common features in terms of chemical bonding. The estimate of the magnetic moment is consistent with the experimental observations, and indicates that the manganese compounds have a high-spin ground state.

I. INTRODUCTION

Ternary hydrides based on transition and alkali or alkaline-earth metals have recently been discovered.[1,2] For these kinds of materials both covalent and ionic bondings coexist. The covalent bonding results from a hydrogen–transition-metal interaction, while the ionic one involves a hydrogen-alkali or alkaline-earth interaction. This leads to a variety of electronic properties going from insulators to metallic conductors. In addition, some such compounds, like intermetallic Laves phase hydrides, exhibit interesting magnetic properties. Much effort has been devoted to the development of preparation techniques and the crystallographic characterization of these materials. However, the physical properties of the ternary hydrides still have to be studied. Particularly interesting among the latter ones are compounds of the general formula A_3TH_5 ($A=K$, Cs, Rb; $T=$Mn, Zn).[3–5] They are all isostructural, and belong to the body-centered-tetragonal (bct) I_4/mcm space group. Recently, Bronger, Hasenberg, and Auffermann synthesized the manganese series of hydrides and deuterides A_3MnY_5 ($A=$K, Rb, Cs; $Y=$H, D).[3,4] They made a crystallographical characterization and measured magnetic properties for all these compounds. These hydrides exhibit a paramagnetic phase, which orders into an antiferromagnetic one at temperatures below 40, 15, and 5 K, for K_3MnH_5, Rb_3MnH_5, and Cs_3MnH_5, respectively. The magnetic structures were determined by magnetic-susceptibility and elastic neutron-diffraction techniques. Spin orientations and local magnetic moments for manganese atoms were obtained. It is interesting to note that such magnetic transitions are not correlated with structural transitions. On the other hand, isostructural manganese halides such as Cs_3MnCl_5,[6,7] as well as the chloride Cs_3CoCl_5, have been extensively studied by both x-ray and (polarized) neutron-diffraction techniques.[8–10] Yvon, Bortz, and Fischer[5] discovered the first example of these kind of hydrides based on Zn metal (K_3ZnH_5), which is presumably nonmagnetic.

In the last few years we have successfully applied *ab initio* techniques to the study of the electronic structure of a variety of ternary hydrides based on transition metals and alkaki or/and alkaline-earth metals.[11–15] Mg_3MnH_7 has recently been studied experimentally.[16] This hydride is formed by octahedral MnH_6 units stacked along the c axis of a primitive hexagonal lattice with Mg atoms inserted between the units. Dimerized Mg_2H chains are located along the c axis. We found that this hydride is an insulator with an indirect energy gap of 2.56 eV opening between the Γ and $M\vec{k}$ points of the hexagonal Brillouin zone.[17] Experimentally, this hydride was found to be a diamagnetic material[16] which is consistent with d^6 low-spin $[MnH_6]^{5-}$ units.

The study of the electronic properties of the series of isostructural compounds A_3TX_5 ($A=$K, Cs, Rb; $T=$Mn, Zn; $X=$H, Cl) allows for an investigation of the role played by hydrogen and chlorine on the bonding of the transition-metal–hydrogen (chlorine) units. In addition, the zinc-metal-based hydride, although being a filled d shell compound, allows for a comparison of the electronic structure between magnetic and nonmagnetic isostructural varieties.

In this work, we use the full-potential linear-augmented-plane-wave (FPLAPW) method.[18] We calculate *ab initio* the spin-polarized energy bands over a large sample of $\vec{k}$ points of the irreducible wedge of the Brillouin zones. The form for the local-spin-density approximation used is the one proposed by Perdew and Wang.[19] The energy cutoff, represented by $R_{MT}K_{max}$ in this method,[20] was set in order to insure convergence to 0.001 Ry in the energy eigenvalues. The total density of states (DOS) as well the partial-wave symmetry analysis of the DOS at each atomic site were computed by means of the tetrahedron integration scheme. For all calculations described in Sec. II the reported charge population analysis was obtained by a direct integration of the total and partial DOS's up to the Fermi energy. The values of the energy gap reported are only indicative due to the uncertainty in their determination. This comes from the inability of the local-density approximation-based methods to predict this property quantitatively. In what follows we present our results for the energy bands and electronic density of states for the elemental high-temperature manganese phases and the series of ternary compounds K_3MnH_5, Cs_3MnH_5, Cs_3MnCl_5, and K_3ZnH_5.

II. BAND-STRUCTURE RESULTS

In order to outline the band-structure results for the manganese hydrides and chloride, we first show our results for

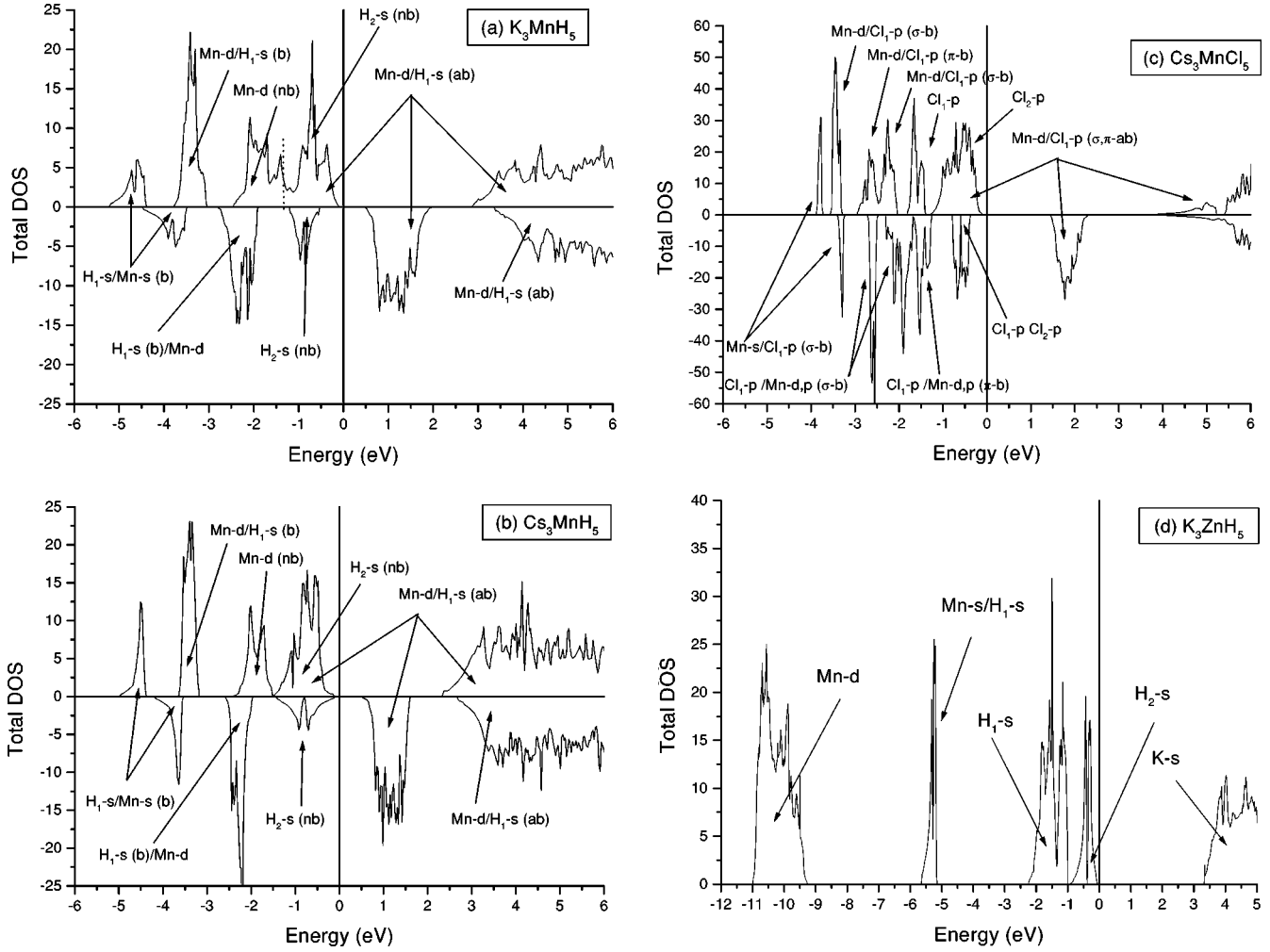

FIG. 1. Total density of states (in states of each spin per eV unit cell) as a function of energy for (a) K_3MnH_5, (b) Cs_3 MnH_5, (c) Cs_3MnCl_5, and (d) K_3ZnH_5. For each structure appearing in the total DOS, the most important orbital contributions are labeled. Here b stands for bonding, ab for antibonding, nb for no bonding, and σ and π hold for symmetry-type bonding. Each unit cell contains two chemical formulas A_3TX_5.

the high-temperature phases of elemental manganese in the face-centered-cubic (fcc) γ-Mn and body-centered-cubic (bcc) δ-Mn structures.[21] These calculations were performed with the FPLAPW method within the above-mentioned approximations for both the exchange and correlation energies. We computed the energy bands and the total and partial DOS's for both γ-Mn and δ-Mn metals. These results were obtained by computing *ab initio* energy eigenvalues over a sampling of 258 $\vec{k}$ points of the irreducible wedge of the Brillouin zones, and by considering the experimental lattice parameters.[22]

TABLE I. Lattice parameters for the tetragonal lattice (a and c), transition-metal–hydrogen (halide), and transition-metal–transition-metal distances (in Å, T=Mn, Zn, X=H, Cl).

	a	c	$d(T\text{-}X)$	$d(T\text{-}T)$
K_3MnH_5 (Ref. 4)	7.519	11.672	1.802	5.317
Cs_3MnH_5 (Ref. 4)	8.234	12.530	1.768	5.822
Cs_3MnCl_5 (Ref. 6)	9.21	14.97	2.347	6.512
K_3ZnH_5 (Ref. 5)	7.5819	11.1671	1.655	5.361

Spin polarization appears clearly from the total and partial DOS plots. The charge population analysis yields to a magnetic moment of $1.90\mu_B$ and $1.29\mu_B$ for γ-Mn and δ-Mn, respectively. This agrees with previous estimates ($1.26\mu_B$ and $1.24\mu_B$)[22–24] for the magnetic moments of the bcc phase. Results for δ-Mn, as previously indicated,[25] are consistent with a low-spin ground state. We found, for γ-Mn, that the magnetic ground state should also be a low-spin one. For γ-Mn we found approximate spin splittings (measured from the peak to peak energy distances) of 1.09, 0.98, and 1.77 eV for the *s*, *p*, and *d* electrons, respectively. For the δ-Mn case, these spins splittings are found to be 0.82, 0.93, and 1.36 eV, respectively. These values are consistent with those reported by Fry *et al.*[23] for the bcc phase. According to these authors, the magnetic moment as well as the spin splittings for δ-Mn are very sensitive to lattice parameters. The increasing of lattice parameters, corresponding to an increasing of the $d(T-T)$ distance, favors the *d* and *s* ferromagnetic band splitting.

Some words must be addressed about the muffin-tin (MT) radii selection for the ternary compounds. It basically followed two considerations, namely, closeness to the Shan-

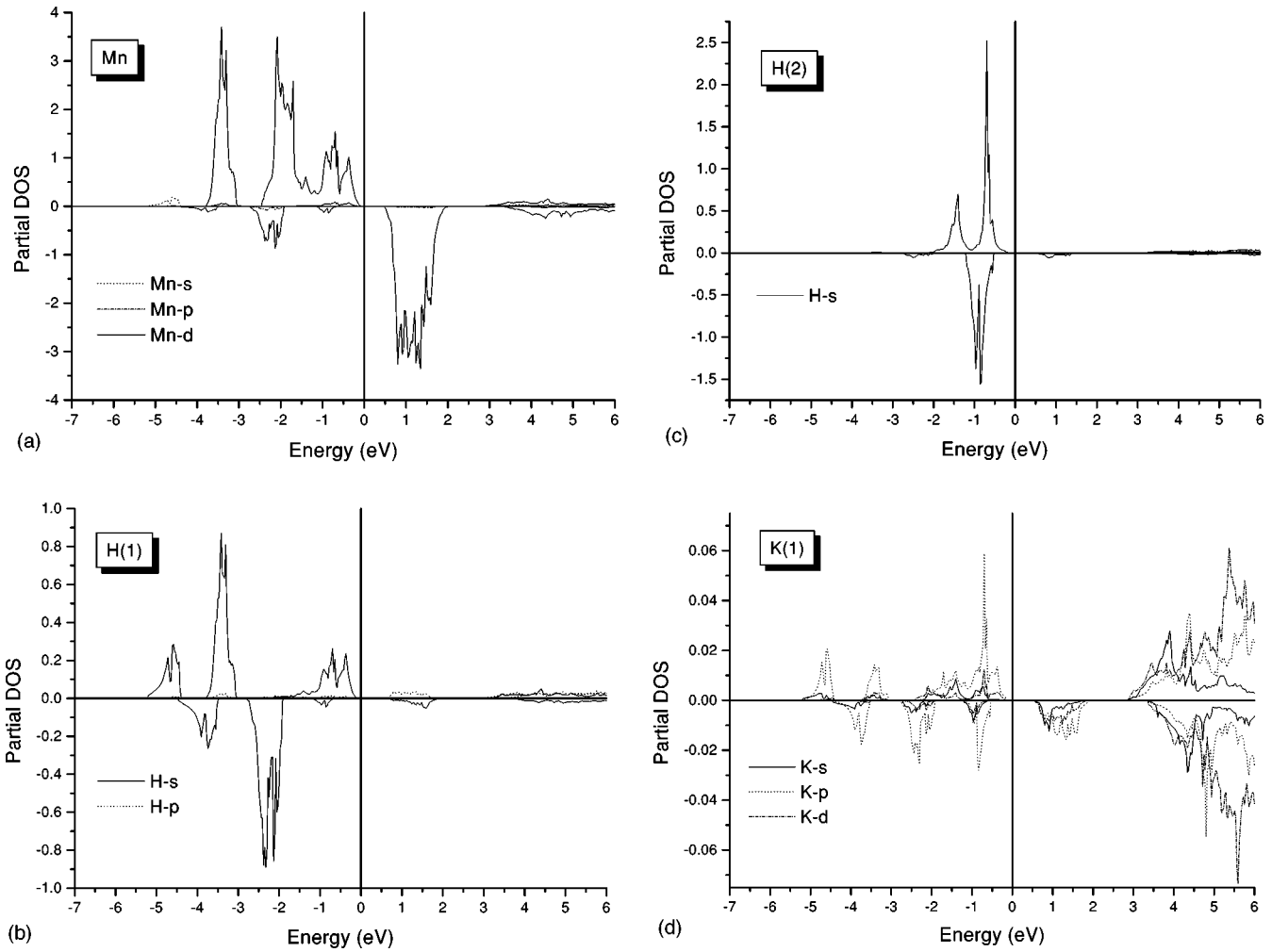

FIG. 2. Partial density of states (in states of each spin per eV atom) as a function of energy for each angular momentum contribution for (a–e) K_3MnH_5, (f–j) Cs_3MnCl_5, and (k–o) K_3ZnH_5.

non's ionic radii,[26] as geometry permits, and preservation of similar MT radii for all elements. Hence we fix the MT radii for the transition metals and hydrogen (chlorine) as half of the *T*-*X* (T=Mn, Zn; X=H, Cl) distance. This gives MT radii for the *T* elements similar to Shannon's values. Geometrical considerations allow for increasing of the alkali-atom MT radii to large values. This does not significantly modify the population analysis when compared with reported values (see Table II) for these *electron donnor* atoms. However, in order to avoid large differences among $R_{MT}K_{max}$ effective atomic values,[20] we set the alkali metal's MT radii as the ones used for the transition metal. Hence the filled *p* states of Mn, Zn, K, and Cs are treated as semicores. These considerations yield the MT radii of 0.90, 0.88, 1.17, and 0.83 Å for each atom in K_3MnH_5, Cs_3MnH_5, Cs_3MnCl_5 and K_3ZnH_5, respectively. These open structures show a large interstitial volume. With the selected MT radii, the interstitial space ranges from 81% to 87% of the cell volume.

In Figs. 1(a)–1(d), the total electronic densities of states for K_3MnH_5, Cs_3MnH_5, Cs_3MnCl_5, and K_3ZnH_5 are shown. To obtain them, *ab initio* energy eigenvalues were computed at 100 $\vec{k}$ points of the irreducible wedge of the bct Brillouin zone. In Table I, we summarize crystal parameters, transition-metal–hydrogen [$d(T$-$H)$] and $d(T$-$T)$ distances for these compounds. These compounds systematically show large $d(T$-$T)$ distances compared to elemental manganese, and short $d(T$-$H)$ distances as in most of the transition-metal hydrides. The manganese atoms occupy the $\bar{4}2m$ (D_{2d}) point-symmetry sites, denoted 4*b* in the Wyckoff nomenclature. The point symmetry of the Mn atom conducts two sets of irreducible representations to describe σ and π bondings. σ bonding maps into $A_1 \oplus B_2 \oplus E$ symmetries. The d_{z^2} and $d_{x^2-y^2}$ atomic orbitals are then of no-bonding character (case of hydrides). However, the π bonding is slightly complicated, since it includes the B_1 symmetry and allows for bonding the d_{z^2} and $d_{x^2-y^2}$ atomic orbitals (the case of chlorides). By simple electronegativity arguments, we should expect a strong covalent character for the Mn-H bond ($\approx$85%) and a somewhat weaker for the Mn-Cl one ($\approx$63%). This crude analysis is consistent with the *charge acceptor* nature of chlorine atoms. State-of-the-art quantum-chemical calculations[27] indicate that the π-back donation mechanism, usually present in the stabilization of transition-metal coordination complexes, is weak when chlorine is the ligand atom, and obviously nonexistent in hydrides. Thus, we expect some qualitative differences in the electronic structure of these compounds, particularly for the weak π

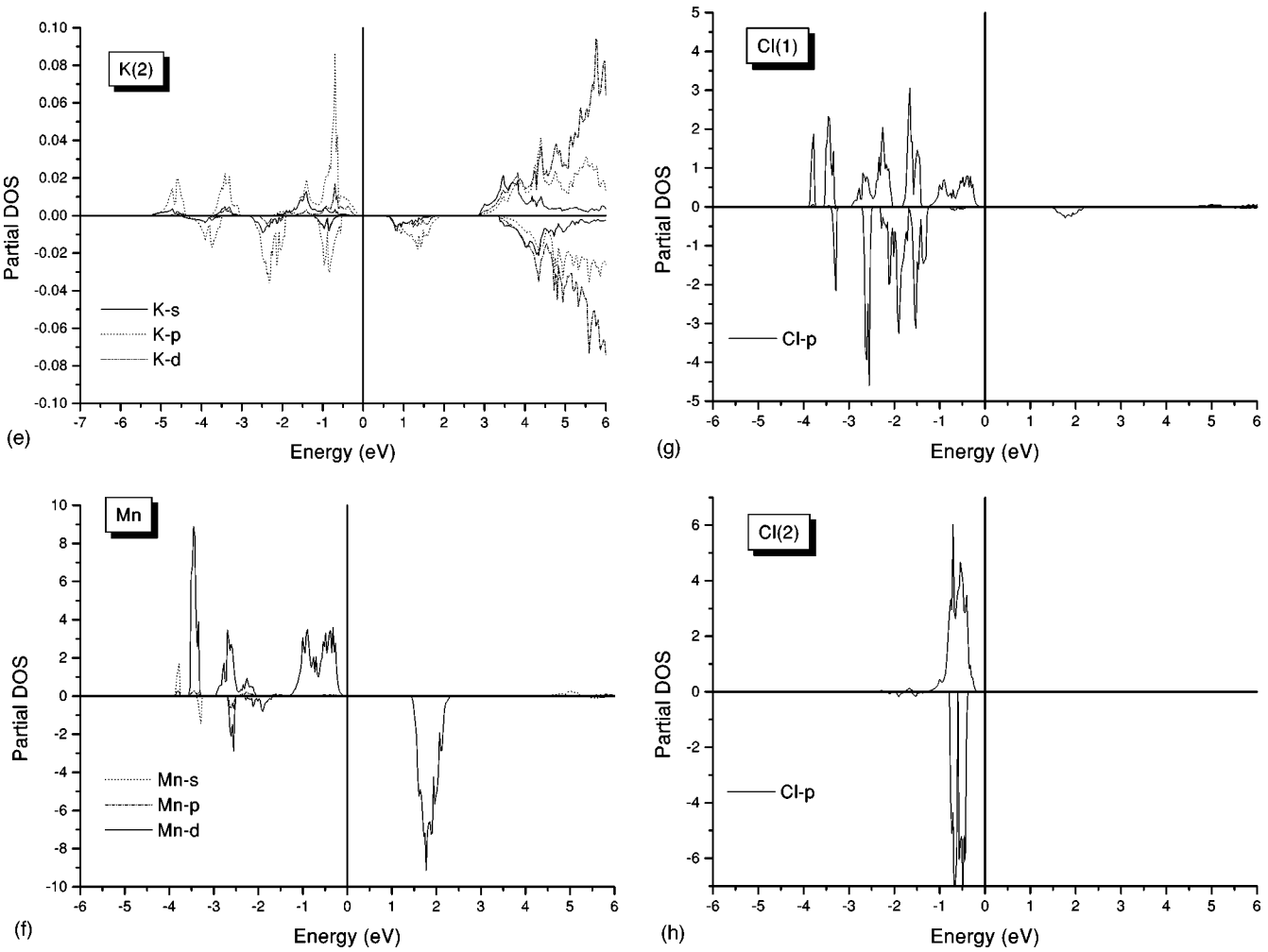

FIG. 2. (*Continued*).

bonding in the chloride, for which ionicity should be more important than in the corresponding hydride. This view can be supported by the analysis of the diffuse neutron-diffraction experiments in the parent compound Cs_3CoCl_5.[8–10] For the latter, the electronegativity analysis indicates, for both cobalt hydride and chloride, a covalency stronger than the one of the manganese compounds.

For K_3MnH_5 we observe, in the spin up plot of the total DOS [Fig. 1(a)], three structures below the Fermi energy, covering an energy range of 5.27 eV. The first structure, at the bottom of the energy scale, is 0.90 eV wide and essentially concerns the $H_{(1)}$-*s*/Mn-*s*/K-*s* and -*p* bonding interactions of a_1 symmetry, as can be appreciated in the partial DOS plots of Fig. 2(a). This structure contains one electron per chemical formula. At higher energies, a structure 1.09 eV wide appears, and is characterized by the Mn-d/$H_{(1)}$-*s* bonding orbital interactions filled with three electrons. In this energy range the wave-function coefficients (not shown) at the center of the bct Brillouin zone (Γ) indicate that the bonding interaction between the Mn-d_{xy}/$H_{(1)}$-*s* orbitals and the doubly degenerate Mn-d_{xz}-d_{yz}/$H_{(1)}$-s orbital is dominant.

At higher energies, closer to the Fermi level, a large and complex structure appears which is composed by the no-bonding states Mn-$d_{x^2-y^2}$ and Mn-d_{z^2}. A large peak at around -0.7 eV is mainly due to the $H_{(2)}$-*s* no-bonding states, while the peak at -2.3 eV concerns the antibonding counterpart of the Mn-d/$H_{(1)}$-*s* interactions. Both substructures are filled with three electrons each. In Fig. 1(a) a vertical dotted line indicates the separation among substructures. Well above the Fermi energy (2.84 eV), for the same spin, the remaining antibonding states Mn-d/$H_{(1)}$-*s* appear.

The analysis for the spin-down part of the total DOS shows three structures. The first one is 1.03 eV wide and, as in the case of the spin-up part, concerns the bonding Mn-*s*/$H_{(1)}$-*s*/*K*-*s* and -*p* states. This structure is also filled with one electron per chemical formula. At higher energies, the second structure, containing three electrons, is 0.95 eV wide and concerns the weak $H_{(1)}$-*s*/Mn-*d* bonding states. The third structure has essentially no bonding, and has a $H_{(2)}$-*s* character. This is clearly shown in the partial DOS plot of Fig. 2(a–e). This no-bonding structure is filled with one electron. The antibonding part of Mn-d/$H_{(1)}$-*s* states for this spin appears well above the Fermi energy. This structure forms a wide electron empty structure of 1.61 eV.

It is interesting to note that charge depletion toward the spin-up peak indicates a strong spin polarization for this compound. We will come back to this point later. We found K_3MnH_5 (rose colored) to be a semiconductor with an energy gap of 0.50 eV.

The total DOS for caesium manganate is plotted in Fig.

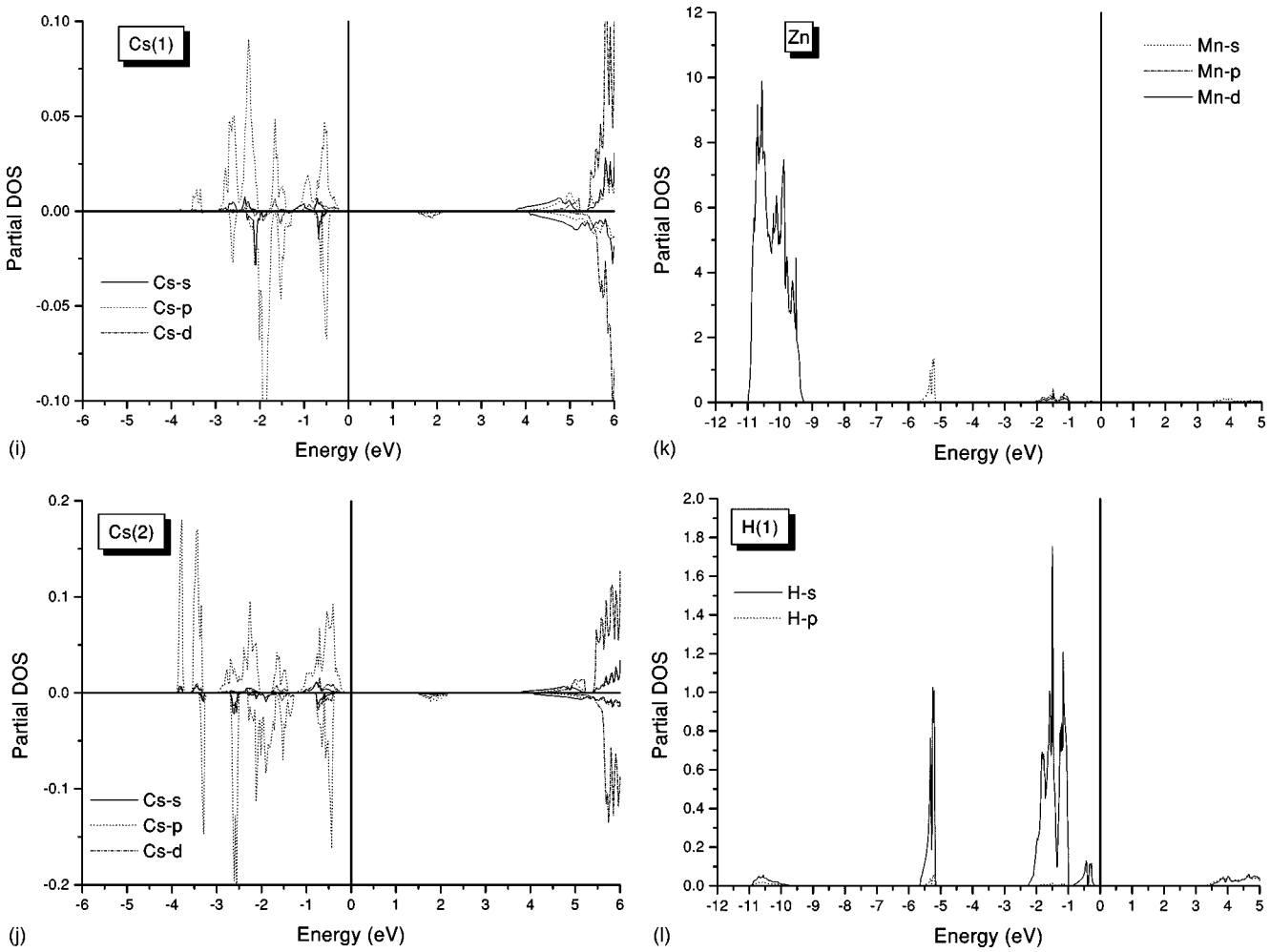

FIG. 2. (*Continued*).

1(b). Here, as in the case of K_3MnH_5, the low-energy bands form narrow structures due to the $H_{(1)}$-*s*/Mn-*s* bonding orbital interactions. The DOS structure concerning the Mn-*d*/$H_{(1)}$-*s*/K-*s* and -*p* is also narrow and, for the spin-up peak, it is separated from the no-bonding $H_{(2)}$-*s* and antibonding Mn-*d*/$H_{(1)}$-*s* interactions. As in K_3MnH_5, the spin-down antibonding Mn-*d*/$H_{(1)}$-*s* states appear above the Fermi energy. The charge distribution among the different DOS structures is similar to the one found for K_3MnH_5. The occupied bands spread over an energy range of 5.03 eV. The energy gap of the greenish-yellow Cs hydride is found to be 0.41 eV.

We found that the bonding-antibonding Mn-*d* energy splitting is similar in both hydrides. In the ternary hydrides M_2FeH_6 (M=Mg, Ca, Sr), of K_2PtCl_6 structure, we have observed that the bonding-antibonding splitting of the transition-metal states increases slightly with cell volume despite the increasing in the $d(T\text{-}H)$ distances.[28,29] In the present case, the cell volume and $d(T\text{-}T)$ distances (see Table I) are larger for Cs_3MnH_5 than for K_3MnH_5. The $d(T\text{-}H)$ distance is smaller for the former than for the latter, and the above-mentioned splitting remains almost constant.

The total and partial DOS's for Cs_3MnCl_5 are displayed in Figs. 1(c) and 2(f–j), respectively. The narrow no-bonding Cl-*s* structure which appears centered at -6.5 eV below the Fermi energy is not shown. In this halide, the nature of the bonding structures appearing in the DOS plot is very complex, and covers an energy range of 3.92 eV. As in the preceding compounds, in the figure we indicate the main orbital contributions to each structure. It can be seen that, for both spins, the low-lying structure is associated with Mn-*s* and $Cl_{(1)}$-*p* of σ-bonding character of a_1 symmetry. For this compound all the manganese *d* orbitals participate in the bonding, as can be seen in the DOS and partial DOS plots. We have pointed out that quantum-chemical calculations do not indicate any important π-electron transfer from the transition metal to the chlorine atoms. However, we found π-orbital interactions in this compound. This is clearly shown in the partial DOS (e.g., in the $Cl_{(1)}$-*p* DOS contributions). For this compound, the charge distribution among the structures appearing in the DOS plot is not easy to identify due to the overlap of the different (σ and π) substructures. Again, for the spin-down peak the Mn-*d*/$Cl_{(1)}$-$p_{\sigma,\pi}$ antibonding contributions are above the Fermi energy. For this greenish-yellow insulator we obtain an energy gap of 1.34 eV.

The electronic structure features of K_3ZnH_5 differ strongly from that of the Mn-based compounds, due to the fact that Zn is a filled 3*d* shell metal. In the DOS plots given in Figs. 1(d) and 2(k–o), we observe a 1.80-eV-wide struc-

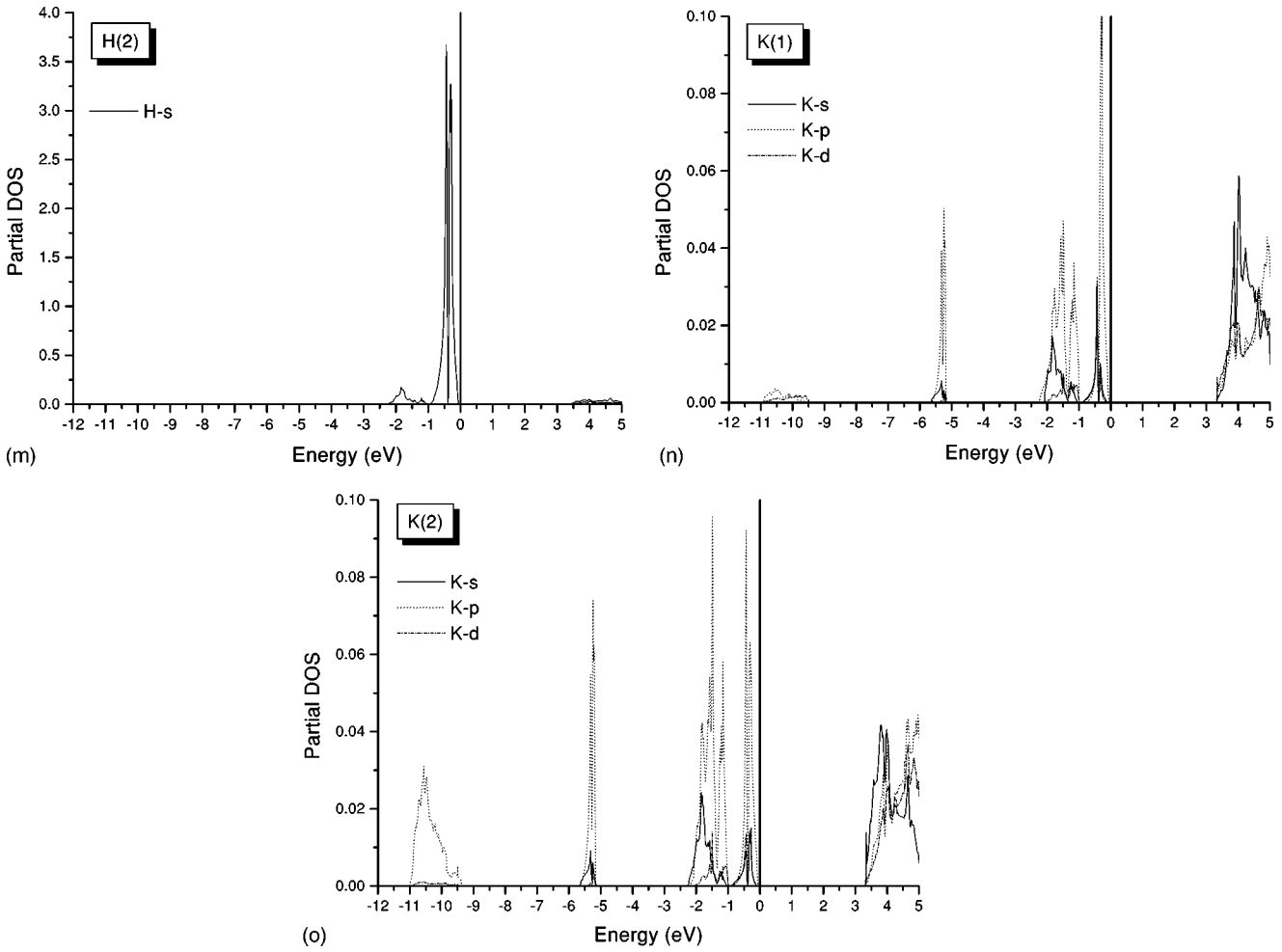

FIG. 2. (*Continued*).

ture, centered at -10 eV. This structure is filled with 20 Zn-*d* electrons. At higher energies, at around -5.7 eV, a bonding Zn-*s*/$H_{(1)}$-*s*/*K*-*s* and -*p* structure of a_1 symmetry appears. At even higher energies, there are structures concerning the almost no-bonding $H_{(1)}$-*s* and the no bonding $H_{(2)}$-*s* structures, as it can be appreciated in the partial DOS plot of Fig. 2(k–o). K_3ZnH_5 is clearly diamagnetic, and shows a large energy gap of 3.29 eV. The values of the energy gap for K_3MnH_5 and Cs_3MnH_5 are too close to each other to extract any clear trend. However, the origin of the energy gap in K_3ZnH_5 is of a different nature. In this *d*-filled band hydride, the value of the energy gap is dominated by the splitting between the bonding and antibonding of the Zn-*s* and K-*s* states.

In Table II we summarize the charge population analysis at each atomic site, resolved by an angular-momentum component. We observe that the Mn-based compounds show a total magnetic moment of $5.0\mu_B$, corresponding to five unpaired electrons. These five unpaired up-spin electrons are clearly related to the *d* states on the Mn site, and other sites are not significantly spin polarized. These results correlate well with the crystal-field value and the observed magnetic-susceptibility measurements.[4] It also indicates the high-spin molecular character of these compounds.[30] Our analysis for the manganese atoms shows local magnetic moments of $1.42\mu_B$, $1.38\mu_B$, and $1.86\mu_B$ for K_3MnH_5, Cs_3MnH_5, and Cs_3MnCl_5, respectively. These values should be handled with care. It should be noted that, for these open structures, the interstitial space is large compared to the *atomic* volumes. As a consequence, a large amount of the total electronic charge is located in the interstitial region, as can be see in Table II. It is interesting to note that for Cs_3MnCl_5, a small spin polarization is found on chlorine atoms. The computed local magnetic moments are $0.05\mu_B$ and $-0.14\mu_B$ for $Cl_{(1)}$ and $Cl_{(2)}$, respectively. Approximate spin splittings were estimated from the projection of the DOS at the manganese site. This was computed by taking the energy distance between the spin-up and spin-down peaks of the Mn-*d* bonding contributions. We obtained 1.1, 1.2, and 0.9 eV for K_3MnH_5, Cs_3MnH_5, and Cs_3MnCl_5, respectively. Results for the magnetic ordered structures are not included in this work. A $2\times2\times2$ supercell *ab initio* study will be reported in the near future.

III. CONCLUSIONS

We have investigated the electronic structure of some of the most representative isostructural A_3TX_5 (A=K, Cs; T=Mn, Zn; X=H, Cl) hydrides and halides. We determined the essential features of the bonding for these compounds.

TABLE II. Population analysis of the valence states at each atomic site resolved by the angular momentum contributions for A_3MnX_5 (A=K, Cs; X=H, Cl). Cl-s states belong to the core and are set to zero.

	K_3MnH_5			Cs_3MnH_5			Cs_3MnCl_5			K_3ZnH_5
	Up	Down	Δq	Up	Down	Δq	Up	Down	Δq	q
Total	10.012	5.003	5.01	10.004	4.968	5.04	20.079	15.060	5.02	14.914
$A(1)$-s	0.003	0.002	0.00	0.004	0.003	0.00	0.002	0.002	0.00	0.005
$A(1)$-p	0.013	0.010	0.00	0.016	0.012	0.00	0.023	0.022	0.00	0.022
$A(1)$-d	0.003	0.001	0.00	0.002	0.001	0.00	0.002	0.001	0.00	0.003
$A(2)$-s	0.004	0.003	0.00	0.005	0.003	0.00	0.003	0.003	0.00	0.007
$A(2)$-p	0.018	0.014	0.00	0.021	0.016	0.01	0.049	0.044	0.01	0.028
$A(2)$-d	0.003	0.002	0.00	0.002	0.001	0.00	0.005	0.004	0.00	0.032
Mn-s	0.032	0.023	0.01	0.029	0.022	0.01	0.062	0.042	0.02	0.105
Mn-p	0.032	0.016	0.02	0.031	0.015	0.02	0.057	0.041	0.02	0.077
Mn-d	1.564	0.170	1.39	1.518	0.172	1.35	2.042	0.225	1.82	4.018
$X(1)$-s	0.234	0.232	0.00	0.226	0.225	0.00	0.000	0.000	0.00	0.419
$X(1)$-p	0.013	0.003	0.01	0.014	0.003	0.01	0.966	0.913	0.05	0.008
$X(2)$-s	0.226	0.225	0.00	0.213	0.214	0.00	0.000	0.000	0.00	0.405
$X(2)$-p	0.000	0.000	0.00	0.000	0.000	0.00	1.812	1.956	−0.14	0.010

The dominating character of the bonding orbital interaction is of direct σ nature between Mn and H or Cl atoms. In the halide, the weak contribution of the lateral π bonding shows a spin polarization that could be detected experimentally. In these Mn-based compounds, the antibonding Mn-d/H-s or Mn-d/Cl-p_σ orbital interactions appear systematically above the Fermi energy for the spin-down contribution. This strong charge depletion produces a magnetic moment, whose estimate is consistent with the one obtained experimentally. This indicates the high-spin character of such materials. We hope that this work will stimulate further experimental research on these interesting materials.

ACKNOWLEDGMENTS

I would like to thank DGSCA (Dirección General de Servicios de Cómputo Académico) of UNAM (Universidad Nacional Autónoma de México) for providing supercomputing facilities.

[1] K. Yvon, in *Encyclopedia of Inorganic Chemistry*, edited by R. B. King (Wiley, New York, 1994).
[2] W. Bronger, J. Alloys Compd. **229**, 1 (1995).
[3] W. Bronger, S. Hasenberg, and G. Auffermann, Z. Anorg. Allg. Chem. **622**, 1145 (1996).
[4] W. Bronger, S. Hasenberg, and G. Auffermann, J. Alloys Compd. **257**, 75 (1997).
[5] M. Bortz, K. Yvon, and P. Fischer, J. Alloys Compd. **216**, 39 (1994); **216**, 43 (1994).
[6] J. Goodyear and D. J. Kennedy, Acta Crystallogr., Sect. B: Struct. Crystallogr. Cryst. Chem. **32**, 631 (1976).
[7] Von H.-J. Seifert and G. Flohr, Z. Anorg. Chem. **436**, 244 (1977).
[8] B. N. Figgis, P. A. Reynolds, and G. A. Williams, J. Chem. Soc. Dalton Trans. 2339 (1980).
[9] P. A. Reynolds, B. N. Figgis, and A. H. White, Acta Crystallogr., Sect. B: Struct. Crystallogr. Cryst. Chem. **37**, 508 (1981).
[10] B. N. Figgis, E. S. Kucharski, and P. A. Reynolds, Acta Crystallogr., Sect. B: Struct. Crystallogr. Cryst. Chem. **45**, 232 (1989).
[11] M. Gupta, in *Electronic Structure and Properties of Hydrogen in Metals*, edited by P. Jena and C. B. Satterhwaite (Plenum, New York, 1983), p. 321.
[12] M. Gupta and L. Schlapbach, in *Hydrogen in Intermetallic Compounds*, edited by L. Schlapbach (Springer, Berlin, 1988).
[13] E. Orgaz and M. Gupta, J. Alloys Compd. **240**, 107 (1996).
[14] E. Orgaz, V. Mazel, and M. Gupta, Phys. Rev. B **54**, 16 124 (1996).
[15] E. Orgaz and M. Gupta, J. Alloys Compd. **253**, 326 (1997).
[16] M. Bortz, B. Bertheville, K. Yvon, S. V. Mitrokhin, N. Verbetsky, and F. Fauth (unpublished).
[17] E. Orgaz and M. Gupta (unpublished).
[18] P. Blaha, K. Schwartz, P. Sorantin, and S. B. Trickey, Comput. Phys. Commun. **59**, 399 (1990).
[19] J. P. Perdew and Y. Wang, Phys. Rev. B **45**, 13 244 (1992).
[20] D. J. Singh, *Plane Waves, Pseudopotentials and the LAPW Method* (Kluwer, Boston, 1994).
[21] H. P. J. Wijn, in *Magnetic Properties of Metals*, edited by R. Poerschke (Springer, Berlin, 1991), p. 4.
[22] F. Delbecq, L. Verite, and P. Sautet, Chem. Mater. **9**, 3072 (1997).
[23] J. L. Fry, Y. Z. Zhao, N. E. Brener, G. Fuster, and J. Callaway, Phys. Rev. B **36**, 868 (1987).
[24] N. E. Brener, J. Callaway, G. Fuster, G. Tripathi, and A. R. Jani, Appl. Phys. B: Lasers Opt. **64**, 5601 (1988).
[25] V. L. Moruzzi, P. M. Marcus, and P. C. Pattnaik, Phys. Rev. B **37**, 8003 (1988).
[26] R. D. Shannon, Acta Crystallogr., Sect. A: Cryst. Phys., Diffr., Theor. Gen. Crystallogr. **32**, 751 (1976).
[27] G. Frenking and U. Pidun, J. Chem. Soc. Dalton Trans. 1653 (1997).
[28] E. Orgaz and M. Gupta, Z. Phys. Chem. (Munich) **181**, 1 (1993).
[29] E. Orgaz and M. Gupta, J. Phys. Condens. Matter **5**, 6697 (1993).
[30] The crystal-field magnetic moment is $\mu = g_s\sqrt{S(S+1)}\mu_B = 5.92\mu_B$, with $g_s = 2$ and $S = \frac{5}{2}$.